Novel position sensitive e^+ - e^- detectors for rare nuclear processes

Abstract: Using ENSAR (EWIRA) support we are building a COmpact Positron Electron spectrometer (**COPE**) with strong permanent magnets interleaved with TPC detectors for studying the internal pair creation process of nuclear transitions. The main design parameters are high efficiency, good energy resolution and precise angular reconstruction. This paper describes the aim of the experiments we are plnning to do with such spectrometer, gives a short overview of the previous pair spectrometers, shows the present status of the developments and describes the novel position sensitive e^+ - e^- detectors we are using in the spectrometer for studying rare nuclear processes.

1. Introduction

In order to understand our microcosm, the creation and composition of the matter we are all made of, larger and larger particle accelerators are constructed. The Large Hadron Collider (LHC) is the latest triumph in a century of astonishing physics. At about the same time that LHC discovered the Higgs-like boson, the recent breakthrough in cosmology reveals that a significant part of the Universe is composed of dark (non-baryonic) matter, but the microscopic identity of dark matter remains a deep mystery.

In a recent series of papers the intriguing possibility was explored that the cosmic dark matter may consist of new elementary particles (χ) with masses in the MeV range. In a renormalizable theory, some particle must mediate the $\chi\ \bar{\chi} \rightarrow e^+e^-$ annihilation. The simplest possibility is to introduce a light, spin-1 boson, coupling to both e^+e^- and $\chi\bar{\chi}$ states. The mass of that boson should be comparable to that of the dark matter candidate: 2 $m_\chi \approx M_U$ [1].

Such a gauge boson U was predicted by Fayet [2] more than two decades ago and recently revisited by Boehm and Fayet [3]. It was argued by Boehm et al. [4] and recently by Fayet and Beacom [5] that light dark-matter particles decaying through such bosons into e^+e^- pairs may be the source of the observed 511-keV gamma radiation in the galactic bulge.

Such particles are not excluded by any obvious laboratory measurement or astrophysical observations. Quite on the contrary, in 1988 de Boer and van Dantzig [6] analyzed emulsion data obtained from relativistic heavy ion reactions in which e^+e^- pairs were observed at short but non-zero distances from the interaction vertices. These events were attributed to the emission and subsequent decay of a light neutral boson with a mass of around 9 MeV/c^2 and lifetime of about 10^{-15} s. These parameters fall within the allowed mass–lifetime window: 5 MeV/c^2 $< m_X <$ 20 MeV/c^2, 10^{-16} s $< \tau < 10^{-13}$ s. This finding motivated a search for anomalous Internal Pair Creation (IPC) in transitions between the levels of ^{8}Be and ^{12}C. The IPC was found to be indeed somewhat anomalous in isoscalar magnetic transitions and normal in isovector E1 transitions, This indicates that an isoscalar neutral boson of pseudoscalar $J^\pi=0^-$ or axial-vector (1^+) character is involved [7].

Spectroscopy of IPC has a long tradition [8, 9]. In a wide range of energies and atomic numbers, the internal-pair formation coefficients are fairly high, typically in the order of 10^{-4}-10^{-3} [10]. The measurement of these coefficients offers an effective method for determining the multipolarity of electromagnetic transitions (especially of high-energy and low-multipolarity transitions) [11].

The determination of the multipolarity of the high-energy transitions produced after particle capture reactions might be especially important for nuclear astrophysics to gain deeper understanding of the dynamics of capture processes leading to a more accurate and reliable extraction of the astrophysical S factor and the thermonuclear reactivity [12, 13].

The array was designed to search for deviations from IPC due to the creation and subsequent decay into electron-positron pairs of a hypothetical short-lived neutral boson. Recent results from both underground and cosmic ray experiments suggest that dark matter may be explained by a light boson having a mass of 10 MeV - 10 GeV and coupled to electrons and positrons. There have been several attempts to observe evidence for such particles, using data from running facilities [16–22] or re-analyzing old experiments [23–27]. Since no evidence for their existence was found, limits have been set as a function of its mass and of its coupling to ordinary matter. In the near future, new experiments are expected to extend those limits into a region of couplings and/or masses so far unexplored. It is not widely known, but indications were found for the existance of such a light boson also in some nuclear physics experiments. While anomaly was obsereved in the internal pair production, the overall results were not consistent with the involvement of a neutral boson [29, 30, 7]. However, a limit of $\leq 4.1\times10^{-4}$ was obtained for the boson to γ-ray branching ratio [28–30, 7, 31].

2. Internal Pair Creation (IPC)

Quantum electrodynamics (QED) predicts [8, 9] that the angular correlation between the e^+e^- pairs emitted in IPC peaks at 0° and drops rapidly with the correlation angle (Θ) as shown in Fig. 1.

The above calculations show that the angular correlations at small separation angles are almost independent of the multipolarity of the radiation, whereas at large separation angles, they depend critically upon the multipole order. Thus, it is important to measure angular correlations at large angles.

For E1 and M1 transitions, the formulation by Goldring [15] for the triple differential pair conversion coefficient is used. In the Born approximation for E1 and M1 multipolarities, the differential transition probabilities are

$$\frac{d\Gamma}{d\Omega_+ d\Omega_- dE_+}(\Theta, E_+) = \frac{\alpha}{16\pi^3 k^3} p^+ p^- \left(\frac{4k^2}{(k^2-q^2)^2)} + 2\frac{p_+^2 + p_-^2}{(k^2-q^2)} \pm 1\right) \qquad (1)$$

with the $\pm$ sign equal to - for M1 and + for E1. The parameter $k = E_+ + E_-$ is the pair energy in units of $m_e c^2$, $q = p_+ + p_-$ is the total momentum in units of $m_0 c$ and α is the fine structure constant. The square of the invariant mass of the electron - positron pair,

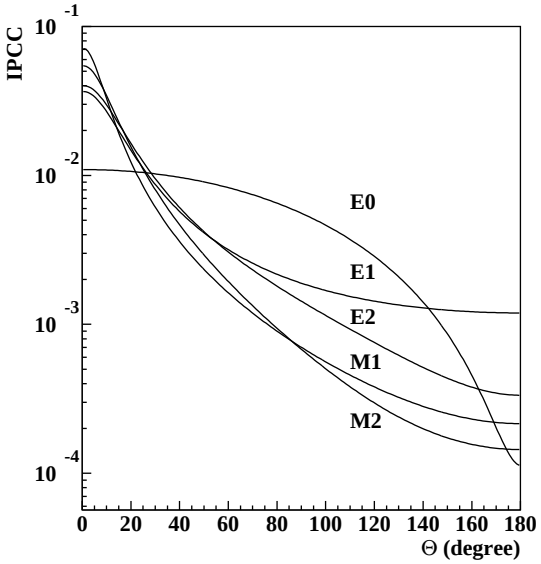

Figure 1: Calculated internal pair conversion coefficients for different multipolarities and a transition energy of E_γ=17 MeV as a function of the correlation angle between the electron-positron pairs.

$\mu^2 = k^2 - q^2$, depends on the opening angle θ according to

$$\mu^2 = 2(E_+E_- + 1)(1 - u * cos(\theta)) \tag{2}$$

where $u = p_+p_/(E_+E_- + 1)$ is close to unity for sufficiently high pair energies. The Θ dependence of the differential pair conversion coefficient in equation (1) is mainly determined by the second term and is similar for E1 and M1 transitions over a wide range of correlation angles. It has the approximate shape of $(1 + cos(\theta))^{-1}$. For E0 transitions, the differential production cross-section for pair conversion can be written in first order as:

$$\frac{dP}{dE_+ dcos(\theta)} = \frac{1}{2}\frac{dP}{dE_+}(1 + \epsilon\cos(\theta)) \tag{3}$$

Where ϵ is an anisotropy factor, given in Born approximation for light nuclei by

$$\epsilon = \frac{p_+p_-}{E_+E_- - 1}. \tag{4}$$

3. The two-body decay of a boson

When a nuclear transition occurs by emission of a short-lived ($\tau < 10^{-13}$ s) neutral particle, the annihilation into an e^+e^- pair is anti-parallel (i.e. $\Delta\Theta_{cm}$ =180°) in the center of mass system. In the laboratory system, their angular distribution is peaked ($\Delta\Theta < 10°$) at intermediate angles due to the Lorentz boost and provides a unique signature for the existence and a measure for the mass of an intermediate boson. In order to search for

such an anomaly in the angular correlation, we need a spectrometer with high angular resolution.

The invariant mass can be determined approximately from the relative angle Θ between e^+ and e^- and from their energies in the following way[30]:

$$m^2 \approx (1-y^2)E^2 \sin^2(\Theta/2), \tag{5}$$

where $E = E^+ + E^- + 1.022$ MeV is the transition energy and $y = (E^+ - E^-)/(E^+ + E^-)$, with $E^{+(-)}$ indicating, respectively, the kinetic energy of the positron (electron) in the laboratory system.

4. Short overview of previous pair spectrometers

A number of instruments used formerly for internal pair studies were magnetic β-ray spectrometers [32–36]. With the aid of an intermediate-image spectrometer and a statistical-separation detector [34, 36] a pair-line efficiency of about 10^{-4} was achieved at the maximum transmission settings. A typical pair-line resolution of 1.3% (in momentum) corresponds to a pair-line efficiency of only 5×10^{-6}. An important advance [35] in the use of intermediate-image pair spectrometers was provided by the installation of a specially designed spiral baffle system, which selected electron-positron internal pairs emitted at large relative angles ($50^\circ \leq \theta \leq 90^\circ$).

The next generation of internal-pair spectrometers used two $dE/dx + E$ scintillator-detector telescopes for the detection of the electron-positron pairs in quadruple coincidence [37, 38]. A multi-detector (six scintillation electron telescopes plus an annular Si(Li) particle detector), high-efficiency pair spectrometer was built by Birk and co-workers [39]. An experimental pair-line efficiency of 28% and a sum-peak energy resolution of 12% for the 6.05 MeV E0 pair line in ^{16}O were achieved.

Schumann and Waldschmidt have detected internal pair spectra in the energy range of 2.8-6.5 MeV from an (n,γ) reaction with the combination of a super-conducting solenoid transporter plus Si(Li)-detector spectrometer [40]. The pair-line efficiency of the spectrometer [41] was large, but it had very limited discrimination power for different multipolarities in this energy region.

The Debrecen superconducting solenoid transporter plus two-Si(Li)-detector electron spectrometer was also adapted for internal-pair studies [42]. The observed pair-line efficiency for two detectors – operated in sum-coincidence mode – was 35%, while the energy resolution was 0.6% at 2 MeV. A similar spectrometer was built by Kibédi and co-workers [43] and has been used recently for internal pair studies [44].

A highly segmented phoswich array of plastic scintillators was constructed for measurements of e^+e^- pairs emitted in high-energy electromagnetic transitions in nuclei by Montoya and co-workers [45]. Electron (and positron) energies of 2-30 MeV can be measured by each individual element, with a total transition energy resolution of δE/E = 13% for a 20 MeV transition. The array covers 29% of the full solid angle and its efficiency is 1.6% for a 6 MeV $E0$ internal pair decay, and 1.1% for an 18 MeV $E1$ transition.

A positron-electron pair spectroscopy instrument (PEPSI) was designed to measure transitions in the energy region of 10-40 MeV by Buda and co-workers [46]. It consists of $Nd_2Fe_{14}B$ permanent magnets forming a compact 4π magnetic filter consisting of 12 positron and 20 electron mini-orange-like spectrometers.

A $\Delta E - E$ multi-detector array was constructed by Stiebing and co-workers [47] from plastic scintillators for the simultaneous measurement of energy and angular correlation of e^+e^- pairs produced in internal pair conversion (IPC) of nuclear transitions up to 18 MeV. The array was designed to search for deviations from IPC stemming from the creation and subsequent decay into e^+e^- pairs of a hypothetical short-lived neutral boson. The angular resolution of the spectrometer determined by the solid angle of the telescopes was $\Delta\Theta = 15^\circ$, while the efficiency for one pair of telescopes was $\approx 3 \times 10^{-5}$. The investigated angular range was extended from 20° to 131°.

In this paper, we present a novel e^+e^- pair spectrometer having remarkably higher efficiency and better angular resolution than previously obtained by Stiebing and co-workers [47].

5. General considerations for building a novel e^+e^- spectrometer

In order to investigate deviations from normal internal pair conversion, a thorough understanding of the apparatus and its properties has to be achieved and demonstrated. Therefore, extended simulations and calibration procedures have to be performed during several stages of the construction of the spectrometer. The simulations were performed with the GEANT code from CERN [53]. Besides the IPC process, the background of γ-radiation, external pair creation (EPC) and multiple lepton scattering was also be considered.

The transportation of the electrons and positrons by different magnetic fields to some solid state detectors, which measure their energies precisely, has been investigated widely in the literature. However, if the energy of the detected electrons increases, the performance of such spectrometers drops rapidly. We have made MC simulations for a very simple geometry by assuming circular detectors with a diameter of 10 cm and thicknesses of 1.5, 3.5 and 10 cm for Ge, Si, and plastic scintillation detectors, respectively. The electron source was placed at 10 cm from the surface of the detectors. Although the thickness of the detectors was larger than the range of the electrons, a lot of the radiation, mostly bremstrahlung created by the slowing down electrons, escaped from the detectors. It turned out that the full-peak efficiency of the detectors drops rapidly, especially for detectors made of materials with larger atomic numbers (ϵ(Ge, 15 MeV) = 4 % as shown in Fig. 2). For high-energy electrons the advantages of the solid-state detectors cannot be used any more.

In particle physics another approach is used. The charged particles are bent in magnetic fields and their bending radius is measured by special tracking detectors. An example of this idea is realized recently at the largest spectrometer of the World, at the ATLAS Experiment at the CERN Large Hadron Collider. The details of the spectrometer are published [54] and also the software is available. The high technology used at

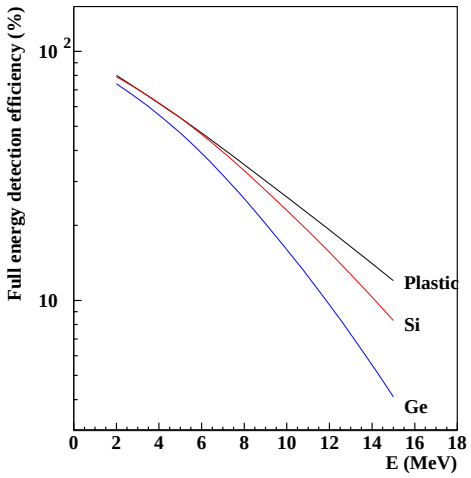

Figure 2: Full-energy peak efficiency of a few detectors as a function of the electron energy

many parts of the spectrometer impressed us very much. That was the reason we started to dream about a small, compact positron-electron spectrometer using toroidal magnetic field, which could be used for studying the internal pair creation of nuclear transitions and which is 100 times smaller than the ATLAS detector.

Nowadays, the methods for tracking minimal ionizing particles have been improved, their electronics and data acquisition systems have been simplified, so we could aim at building a novel positron-electron spectrometer by using the above mentioned idea even in smaller size nuclear physics laboratories. We could make use of the advantages of the strong ($Nb_2Fe_{14}B$) permanent magnets also for creating sufficiently strong magnetic fields for bending 10 - 20 MeV electrons and positrons.

6. A Compact Positron Electron Spectrometer

We proposed to build a COmpact Positron Electron spectrometer (**COPE**) with permanent magnets interleaved with tracking detectors for studying the internal pair creation process of nuclear transitions. The main design parameters are high efficiency, good energy resolution and precise angular reconstruction. Using strong permanent magnets and MICROMEGAS (MICRO-MEsh-GAseous Structure) type tracking detectors [55], the sizes of such a spectrometer can be limited to a diameter of about 30 cm and a length of about 20 cm.

The MICROMEGAS detector operates as a two-stage parallel plate avalanche chamber. It has definite advantages compared to the formerly used multiwire proportional chambers (MWPC) [53]. Its spatial resolution is not limited by a wire spacing of 1 mm, and it is especially suitable for high-rate applications. In the Micromegas detector the wire plane is replaced by a thin electroformed micromesh. The amplification occurs between the mesh plane and a microstrip plane. This small gap, of about 100 μm, between the anode and cathode planes is kept by precise and insulating spacers.

The geometry of the spectrometer is shown schematically in Fig. 3.

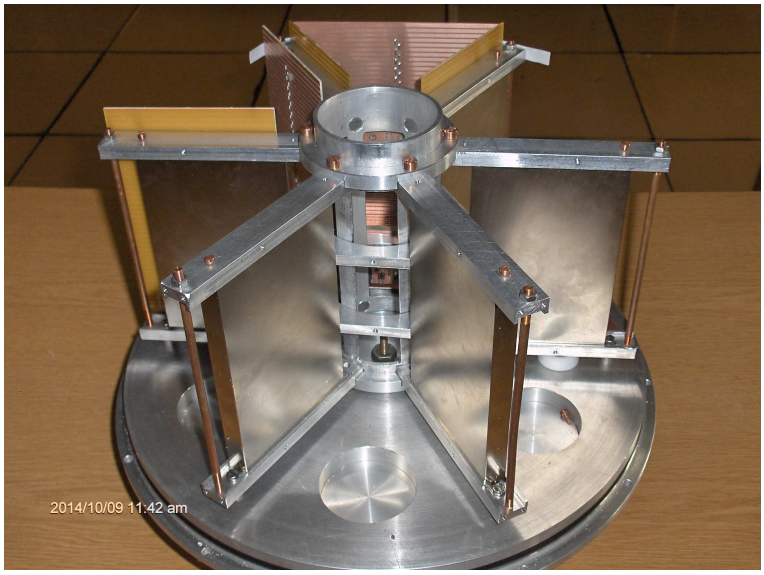

Figure 3: Geometrical arrangement of the NdFeB permanent magnets (from NEOTEXX Company, Germany) of the COPE spectrometer. The sizes of the magnets: 150 mm x100mm x 15 mm

A toroidal magnetic field is maintained by permanent magnets. The magnetic field distribution was calculated by the PerMag 6.5 code (http://www. fieldp.com). Inside the gaps the magnetic field of 0.3±0.1 T is reasonably homogenous as shown in Fig 4.

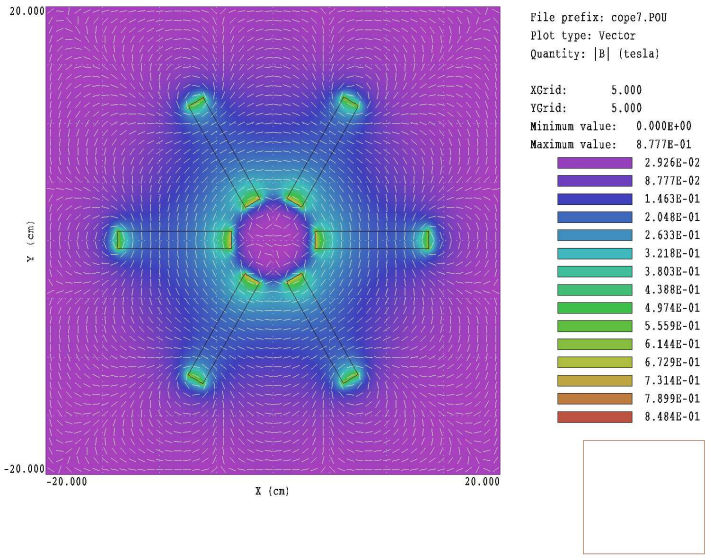

Figure 4: Magnetic field calculations for the COPE spectrometer

By assuming homogenous magnetic field inside the gaps, a few electron paths corresponding to energies of 5, 5.5, 10, 11, 15 and 16 MeV inside one of the gaps of the

spectrometer are shown in Fig. 5. Even at the highest energies the separation of the orbits is reasonably large (≈3 mm for electron energies of 10 % difference) so if we assume an accuracy for the position measurement of 0.15 mm, than an energy resolution of better than 1 % can be achieved. This energy resolution is about 10 times better than we have presently with plastic scintillation telescopes. The solid angle covered by the spectrometer can be as large as 2π.

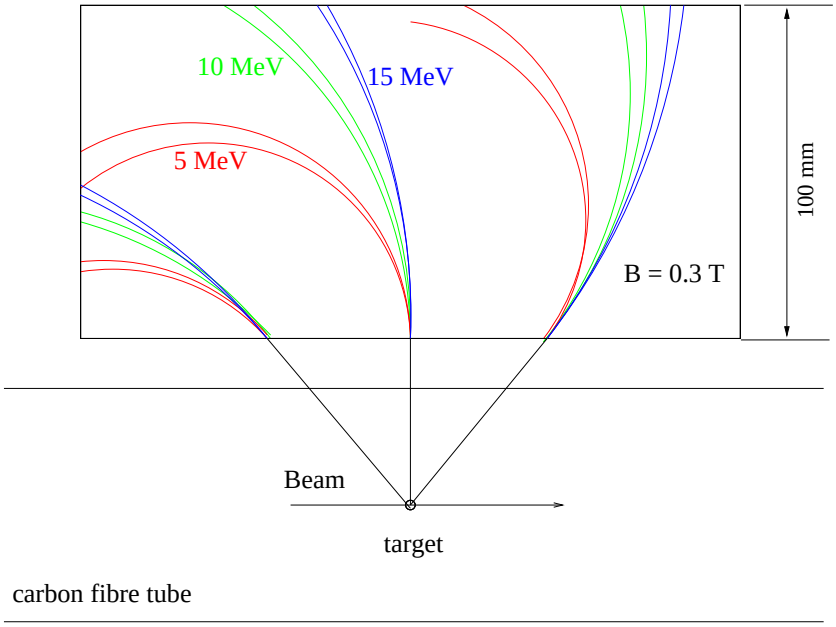

Figure 5: A few electron paths in the magnetic field of the COPE spectrometer.

The magnetic field has been measured inside the gaps by using a Hall probe. Some of the results are shown in Fig. 6,7, 8.

The target will be situated in the center of the detector barrel in a vacuum chamber with a diameter of about 7 cm and a very thin wall of 50 mg/cm^2. In order to minimize the effect of the external pair creation the target frame and holder will be very thin. Two detector layers just outside the chamber would determine both the position and approximate angle of incidence for the electrons and positrons before entering into the toroidal magnetic field created by the permanent magnets. The outer detector layers will be positioned inside the magnetic field to determine the bending radius and the momenta of the particles. Precise mapping of the magnetic field is certainly crucial for the best results. The final parameters of COPE was further optimized by GEANT simulations of its response.

During the design period the idea of the TPC concept and its readout has been evolved. Considering an economic solution, the following concept was accepted. The trajectories of the electrons and positrons are measured by six similar time projection chambers (TPC). Small TPCs have been developed recently in many laboratories for electron tracking Compton imaging used in MeV gamma-ray astronomy. We are planning to use the idea of such devices in each gaps of the COPE spectrometer for detecting the three-dimensional

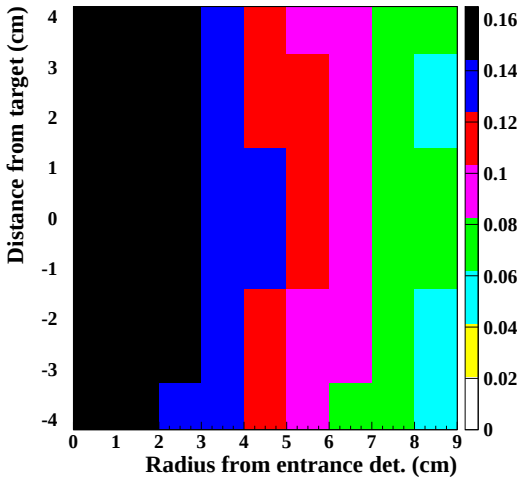

Figure 6: Measured magnetic field distributions at the middle of the gaps as a function of the distance from the central detector and the vertical height measured from the target position (http://www.fieldp.com, PerMag 8.0)

electron-positron tracks. The working principle of one trapezoidal detector is shown in Fig. 9.

In this case a relative small number of pads (and associated electronics) are used and the curvature information for the trajectories comes mainly from the drift times.

The B magnetic field created by the strong permanent magnets, bends the trajectories of the detected particles. The homogeneous electric field is created by a field cage realized by copper strips configured on conventional G10 material surrounding the whole volume of the detector and interconnected by a resistor chain as shown in Fig. 10. The good isolation of the detector box will be carried out by Teflon covering sheets. Different filling gas mixtures has been considered, which provides a drift velocity of about 5 cm/μs at 100-200 V/cm and gives good lateral resolution (FWHM$\approx$0.6 mm), which is important for the precise determination of the curvature of the tracks. The electron clouds created along the curved trajectories of the high energy electrons will drift towards a triple gas electron multiplier (GEM), which provides the proper charge amplification (10000). (We choosed GEM's instead of MICROMEGAS as it is easier to handle.) The amplified charge will then be detected by 40 trapezoidal pads (in each TPC), which are configured at the bottom of the detector box, and which are connected to charge sensitive preamplifiers.

From one electron track we are expecting many pads to be fired along a row of pads as shown in Fig. 9, but only along one raw as the pads are wide enough. In the six detectors we are expecting two tracks (from an electron-positron pair) at the same time. We can afford then to multiplex the analog shaped outputs of the preamplifiers in such a way, that each column of the six detectors 6 x 5 =30 pads will be multiplexed into two outputs. For technical reasons we decided to use 32 channel multiplexers produced by Mesytec (MUX-32). We bought altogether 8 of such multiplexers for the 8 columns, which will

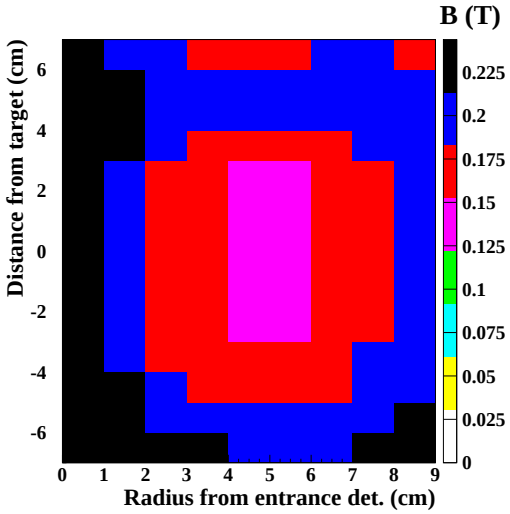

Figure 7: Measured magnetic field distributions close (5 mm) to the magnets

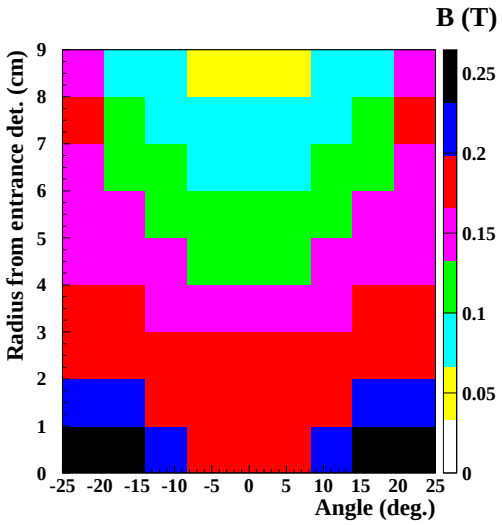

Figure 8: Measured magnetic field distributions between the gaps as a function of the angle and the distance from the central detector

produce 16 energy signals and 16 identification signals. The output of the multiplexers will be connected to a CAEN DT5740 desktop digitizer. The energy as well as the timing of the signals, which determines the drift time and the z coordinate of the tracks will be calculated from the digitized signals.

The chamber of the spectrometer together with the associated electronics can bee seen in Fig. 11.

In the following we will review a few novel position sensitive detectors, which was considered in the designing period of the COPE spectrometer.

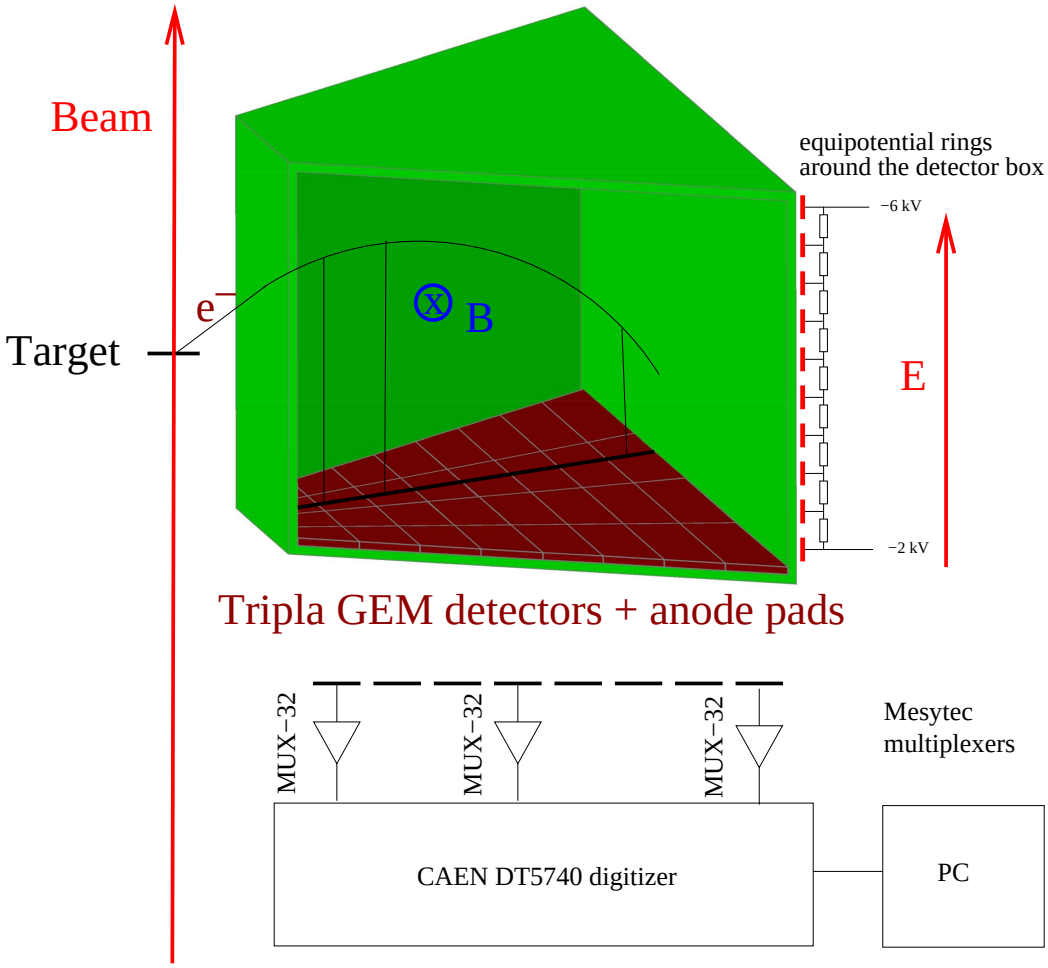

Figure 9: The simplified layout of a TPC detector box. The trajectories of the electrons and positrons are measured by six similar time projection chambers (TPC). Similar electronics will be used, which was developed for DSSSD detectors. Digital data acquisition sytem: http://sourceforge.net/projects/at-vda/

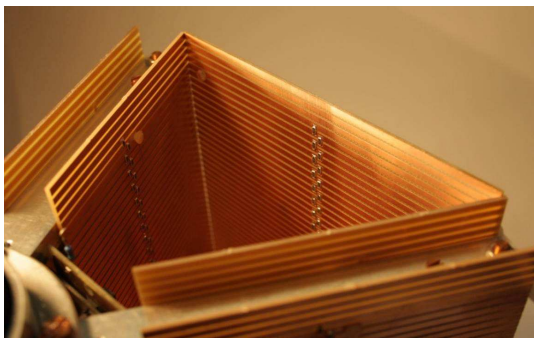

Figure 10: Top view of the completed electric field cages

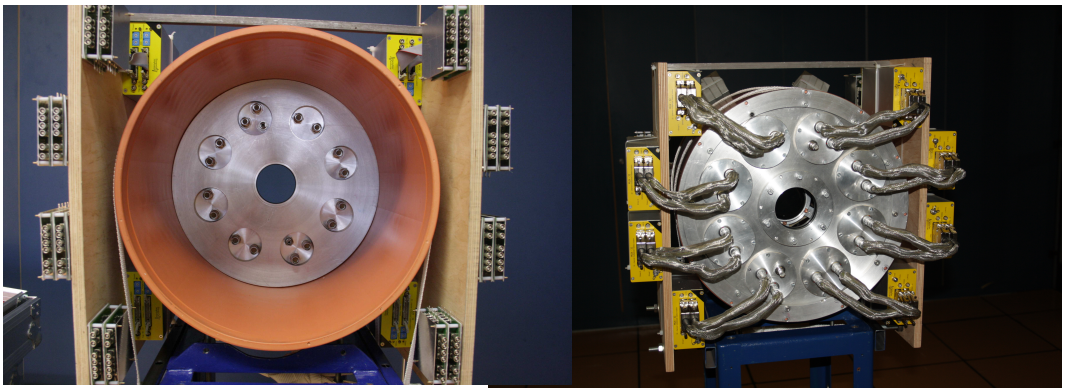

Figure 11: The chamber of the spectrometer with the electric feedthrough and the associated electronics

7. Novel position sensitive e^+ - e^- detectors for rare nuclear processes

Recently, Sauli reviewed the staus of the gaseous radiation detectors [48], which was a good guidance in designing and building the COPE spectrometer.

Multi-wire proportional chambers and drift chambers were developed at CERN during the late 1960s [50, 51]. These devices, together with the parallel development of electronics, were pivotal for a major step forward in particle-detector technology. Its basic concept is simple : Thin anode wires are streched between two cathode foils at high voltage, each wire acts as a proportional counter and amplifies the ionization tracks, released by charged particles crossing the gas in the chamber. They are commonly used in the detection of X-rays, neutrons and charge particles [52, 53] because they can be built in large size, have relatively good energy and position resolution, high efficiency, good uniformity over the sensitive volume and show no radiation damage as compared to the solid state and scintillation detectors.

The advantages of MWPC detectors are well-known. Their sensitive area can be tailored to a variety applications. They are radiation-hard, which is intrinsic to a flushed detector with internal gain. The gain can reach 10^6, making possible to detect minimum ionizing particles with accurate timing and position sensing.

The standard MWPC has also limitations:

- The anode wire spacings determines the resolution normal to the to wire direction; in fact, a resolution substantially smaller than the spacing requires analog information handling. Smaller wire spacings is an obvious route for spatial resolution, lowers the field at the wire, which must be compensated by higher voltages. With spacings smaller than 1 mm, voltages become so high that operation of MWPC becomes difficult.

- Positive ions of relatively low mobility created by the avalanche are almost all collected on the upper and lower cathode strips after a long path in a relatively low field. Hence, the rise-time of pulses is fairly long and the build up of ions around the wires modifies the electric field and the gas gain thus limiting maximum local countrate to 2 x 10^4 /mm/s.

- The wire structure is fragile and subject to ageing.
- The resolution is limited by the parallax effects due to the thick detector.

Despite various improvements, position-sensitive detectors based on wire structures are lim- ited by basic diffusion processes and space charge effects in the gas to localization accuracies around 100 μm. The presence of slow moving positive ions from electron avalanches generates a positive space charge in the drift tube, that modifies electric field and leads to the uncertainty in the space-to-drift time relation. In standard operating conditions, the gain of a MWPC starts to drop at particle rates above 10000 mm^2/s, leading to a loss of detection efficiency. Together with the practical difficulty to manufacture detectors with sub-mm wire spacing, this has motivated the development of new generation gaseous detectors for high luminosity accelerators.

7.1. Micro-Pattern Gas Detectors (MPGD)

Modern photo-lithographic technology led to the development of novel Micro-Pattern Gas Detec- tor (MPGD) concepts, revolutionizing cell size limitations for many gas detector applications. By using pitch size of a few hundred microns, an order of magnitude improvement in granularity over wire chambers, these detectors offer intrinsic high rate capability ($\geq 10^6$ Hz/mm^2), excellent spatial resolution ($\approx$ 30 μm), multi-particle resolution ($\approx$500 m), and single photo-electron time resolution in the ns range.

Owing to the small anode-to-cathode distance ($\approx$ 100 μm), the fast collection of positive ions by nearby cathode strips reduces space charge build-up, and pushes the maximum rate capability of MSGC, compared to MWPC, by more than two orders of magnitude. Despite their promising performance, experience with MSGCs has raised serious concerns about their long-term behavior. There are several major processes, particularly at high rates, leading to the MSGC operating instabilities: substrate charging-up and time-dependent modification of electric field, surface deposition of polymers (aging) and destructive micro-discharges under exposure to heavily ionizing particles. The problem of discharges is the intrinsic limitation of all single-stage micro-pattern detectors in hadronic beams.

In the high fields and narrow gaps, the MSGC turned out to be prone to irreversible discharges induced by heavily ionizing particles and destroying the fragile electrode structure. Nevertheless, the detailed studies on their properties, and in particular, on the radiation-induced processes leading to discharge breakdown, led to the development of mature technologies and novel approaches (GEM and MICROMEGAS) with similar performances, improved reliability and radiation hardness.

7.2. MICRO-Mesh-Gaseous Structure (MICROMEGAS)[55]

This device operates as a two-stage ParalleI Plate Avalanche Chamber (PPAC) with a relatively large (3 mm) conversion/drift gap (the volume between the drift electrode and the micromesh) and a narrow (($\approx$100 μm) amplification gap (the volume between the micromesh and the anode plane). The latter gap is defined by insulating spacers (quartz

fibres) placed between the micro-mesh and the surface of the substratum. This detector is realized in low-cost technology. It has a good granularity and a high and stable gain.

The anode-cathode distance is quite small. Further, the transparency of the micromesh for electrons emitted in the conversion region depends on the ratio of the field strengths in the amplification and in the conversion/drift region; in typical operating conditions, this ratio is large so that the transparency is unity. In contrast, the transparency for ions emitted by avalanches is very weak, as the ratio is inverted. As a consequence, it can be expected – and experiments confirm this view that this device has an extremely high count rate capability.

The advantage of a Micromegas micropattern compared to the wires in the MWPC is robustness and simpler geometry. This insures gain uniformity and good energy resolution.

7.3. Gas Electron Multiplier (GEM)

The GEM foil, short GEM, is a thin insulating polymer foil, coated on both sides with a very thin metal layer. The whole plane is perforated with a large number of circular holes. A standard-design GEM consists of a 50 μm thick Kapton foil covered on both sides with a 5 μm copper layer. The hole diameter in the copper (D) is 75 μm, the center-to-center distance (P) between the holes is 140 μm . The GEMs are produced in the CERN workshop with the help of photolithographic methods. The pattern of the holes is first engraved in the metal surface afterwards etched with a Kapton-specific solvent from both sides. This leads to the double conical shape of the holes, an important factor for the operation of GEMs. The Kapton tips prevent shortcuts between the two electrodes by operating voltages ($\approx$ 400V). The holes have an inner diameter (d), from tip to tip, of 65 μm, slightly smaller than D.

7.3.1. GEMs as Amplification Structure

The Gas Electron Multiplier was developed and produced at CERN by Sauli and his group [43]. A GEM is a 50 μm thin kapton foil coated with 5 μm copper on both sides. Holes with a diameter of 70 μm and a pitch of 140 μm are etched into the foil (cf.Figure 12). By applying a voltage across the GEM a high electric field is created inside the holes where gas amplification is possible. Figure 13 shows a schematic distribution of the electric field lines in such a device. Neglecting magnetic fields and diffusion, the charge carriers travel along these lines. To reach a total gain of about 10^4 with reasonable voltages across a GEM foil, a stack of several, usually three, GEMs is used to amplify the electrons from the primary ionisation process.

7.4. The drift velocity of the electrons and ions created by the fast e^+ - e^- pairs

To describe the drift of the primary electrons through the gas volume, information about the gas properties like drift velocity, longitudinal and transverse diffusion is needed. The program MAGBOLTZ [49] can calculate these properties, taking into account the detailed behaviour of the gas molecules.

The properties of three gas mixtures TDR (Ar/CH4/CO2 93/5/2), P5 (Ar/CH4 95/5) and P10 (Ar/CH4 90/10) have been studied. The calculations were done for a temperature

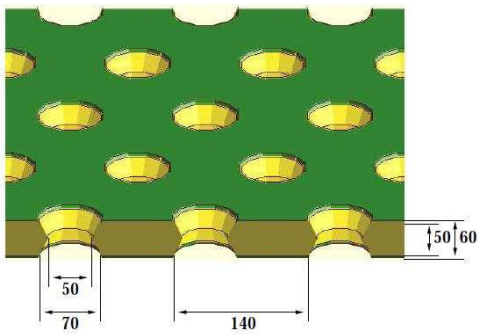

Figure 12: Schematic view of a GEM foil showing the dimensions in μm of the hole size, the pitch and the thickness of the foil.

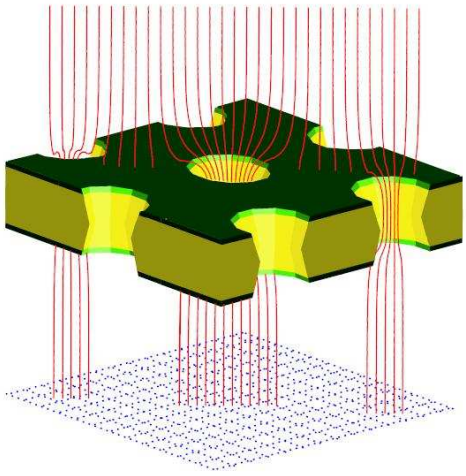

Figure 13: Electrostatic simulation with GARFIELD [44] of electron drift lines in a GEM.

of 295 K and a pressure of 1013.25 hPa. The drift velocity is a function of the electric field E. This dependency is shown in Figure 14.

8. Optimalization of the voltages of the triple GEM detctor

For optimalization of the voltages of the triple GEM detector we have built a test detector set as shown in Fig. 15. The detector was tested with a ^{55}Fe source in a clean room (ISO5, class 100).

Both GEMs and MICROMEGAS should be handled in a clean room with gloves; a facial mask is recommended. They can be glued on supporting fiberglass frames; contact with dirty or hard surfaces should be avoided (found to generate shorts). The simplest assembly procedure for small size GEMs (up to 10x10 cm^2) is to tension-tape the GEMs on a temporary frame and overlay on the (smaller) final frame previously coated with epoxy. If using thin frames, pasting one frame on each side of the GEM eliminates

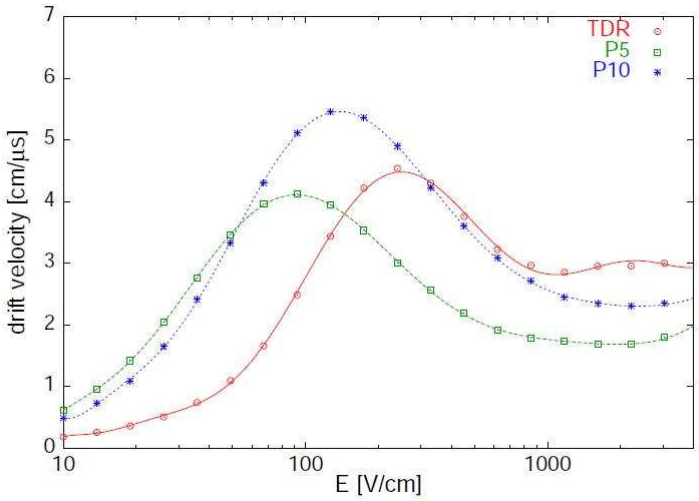

Figure 14: Drift velocity as function of the electric field for different gas mixtures

warping. For larger sizes, the temporary holding frame has to be larger than the final, and weight-loaded to keep the foil under tension during curing. A better procedure is to temporarily paste the GEM outer edges on a sturdy metal or plastic frame and glue on the final frame at controlled high temperature (40 to 50 degrees). This guarantees good mechanical tension of the GEM at room temperature. Special care should be taken to prevent epoxies to diffuse into the GEM holes; it has been found that (even using certified insulating glues) this can substantially increase the leakage current, possibly because of insufficient polymerization or moisture inclusion in the holes.

An important task was the reduction of ions drifting back from the amplification structure into the drift field region of the TPC. These ions would cause field distortion altering the drift velocity and therefore the resolution of the detector. A solution is provided mostly by the intrinsic suppression of ions with multi-GEM structures.

Ions reaching the TPCdrift volume would represent a positive space charge and deteriorate the electric drift field. The ion feedback can be derived from the measurements by dividing the cathode current by the anode current. Highly asymmetric electric fields on both sides of a GEM lead to ion suppression. The small electric field in the drift volume for example, causes many of the drift lines from the amplification region inside the GEM hole to end on the copper plane facing the TPCdrift volume. Therefore, the relatively small drift field typical of a TPC automatically leads to ion feedback suppression. Moreover, the ion feedback can be minimised by the variation of the electrical fields within the GEM structure. Using the TDR gas mixture, we searched for a setting with optimum ion feedback suppression with the drift field constrained at 200 V/cm and requiring an effective gain of 10^4.

- The first two GEMs are set at voltages of 310 V,
- the last GEM at 350 V,

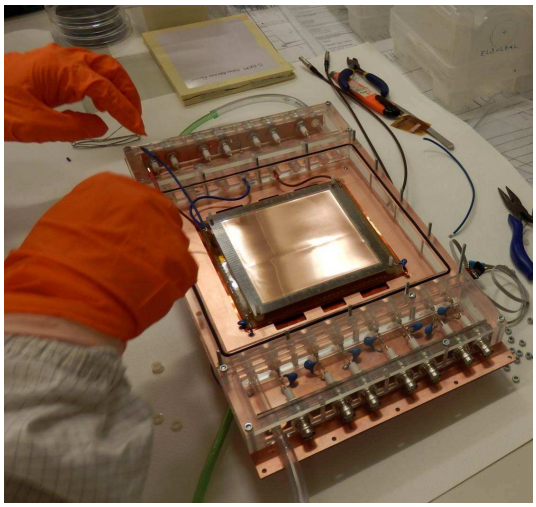

Figure 15: Assembling a test detector with triple GEM's in a clean room

- the first transfer field and induction field are set very high (6000 and 8000 V/cm; respectively,
- whereas the second transfer field is set rather low (60 V/cm).

Using this optimised setting allows a long term and stable operation of a triple-GEM structure with ion feedback well below 1%.

9. Internal tracking detectors

The simplified version of the TPC we pesented before is good for determining the curvature and the momentum of the particles, but for the precise measurement of the angle of incidence and later on the angular correlation of the electron-positron pairs we are using additional tracking detectors at the entrance of the TPC's.

The positions of the hits are measured by conventional MWPC detectors which was constructed at ATOMKI as shown in Fig 16. The anode of the MWPC is a set of parallel 10 μm thick gold-plated tungsten wires at a distance of 2 mm from each other. The two cathodes are composed of copper strips on thin (50 μm) PCB boards separated by 1.27 mm. The anode-cathode distance is 3.5 mm. The two cathodes are placed perpendicularly to each other giving the x and y coordinates of the hit. Delay-line read-out (10 ns/taps) is used for the cathode wires. The accuracy of the (x, y) coordinates implies an angular resolution of $\Delta\Theta \leq 2^\circ$ (FWHM) in the 40°-180° range.

9.1. Beam and Target

To minimize the amount of material around the target, a 24 cm long electrically conducting carbon fibre tube with a radius of 3.5 cm and a wall thickness of 0.8 mm is used. The target, positioned perpendicular to the beam, is held by two perspex rods with a diameter of 3 mm at the side. The rods are arranged parallel to the beam and their

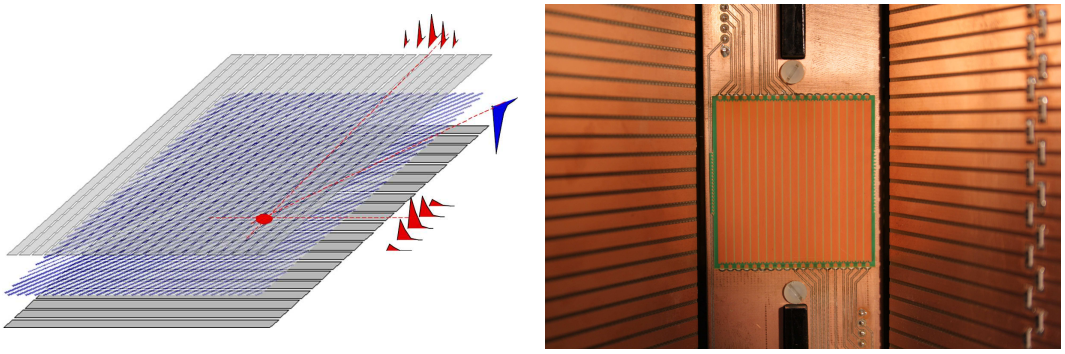

Figure 16: Principle of the MWPC and the construction of the central MWPC detectors and the electric field cages

distance from the beam was 25 mm. On the basis of simulations, they did not cause significant background via external electron-positron conversion. The bars were 12-cm long, and the placement was done so as not to cause any shadowing effects in any of the telescopes. The targets have a typical thickness of 0.3 mg/cm^2, which is adapted to the resonance widths of the reaction under investigation as well as to the demand of a sufficient real-to-random ratio of coincidences. The beam is absorbed in a Tantalum Faraday-cup 15 cm behind the target.

9.2. Conclusion

This COPE spectrometer will be ready in 1-2 months, but some of the experiments we were planning to do with such spectrometer was more urgent, so we constructed a more simple spectrometer by using only the central MWPC detectors and their electronics together with plastics scintillator telescopes. We have already got some nice experimental data with such spectrometer, which will be published soon. The first version of an article, which will be submitted to Nuclear Instruments and Methods is attached to this document.

References

[1] N. Borodatchenkova, D. Chouudrhurly and M. Drees, Phys.Rev.Lett. **96** 141802 (2006).

[2] P. Fayet, Nucl. Phys. B187, 184 (1981).

[3] C. Boehm and P. Fayet, Nucl. Phys. B 683, 219 (2004).

[4] C. Boehm et al., Phys. Rev. Lett. 92, 101301 (2004); Phys. Rev. D 69, 101302 (2004).

[5] P. Fayet, Phys. Rev. D 70, 023514 (2004).

[6] F.W.N. de Boer and R. van Dantzig, Phys. Rev. Lett. 61, 1274 (1988).

[7] F.W.N. de Boer et al., Phy. Lett. B 388, 235. (1996); J. Phys. G 23, L85 (1997); J. Phys. G 27 L29 (2001).

[8] R. Wilson, Internal Pair Formation, in: K. Siegbahn (Ed.), Alpha-, beta- and gamma-ray spectroscopy, Vol. 2, North-Holland Publishing Company, Amsterdam, 1965, Ch. XXV(c), p. 1557.

[9] M.E. Rose, Phys. Rev. 76 (1949) 678. M.E. Rose, Phys. Rev. 78 (1950) 184.

[10] P. Schlüter and G. Soff, At. Data Nuct. Data Tables 24 (1979) 509.

[11] P. Schlüter, G. Soff, W. Greiner, Phys. Rep. 75(6) (1981) 327.

[12] R.M. Chasteler et al., Physical Review Letters, 72 (1994) 3949.

[13] M. Spraker et al., Phys. Rev. C61b(1999) 015802.

[14] M.E. Rose, Phys. Rev. 76, 678 (1949).

[15] G. Goldring Proc.Phys.Soc. A **66** 341 (1953).

[16] H. Merkel, P. Achenbach, C. A. Gayoso et al., Search for light Gauge Boson of the dark sector at the mainz microtron, Physical Review Letters, vol. 106, no. 25, Article ID 251802, 2011.

[17] S. Abrahamyan, Z. Ahmed, K. Allada et al., Search for a new Gauge Boson in electron-nucleus fixed-target scattering by the APEX experiment, Physical Review Letters, vol. 107, no. 19, Article ID 191804, 2011.

[18] J. P. Lees, V. Poireau, V. Tisserand et al., Search for low-mass dark-sector Higgs Bosons, Physical Review Letters, vol. 108, no. 21, Article ID 211801, 2012.

[19] B. Echenard, Search for low-mass dark matter at BABAR, Modern Physics Letters A, vol. 27, no. 18, Article ID 1230016, 2012.

[20] F. Archilli, D. Babusci, D. Badoni et al., Search for a vector gauge boson in meson decays with the KLOE detector, Physics Letters B, vol. 706, no. 4-5, pp. 251255, 2012.

[21] D. Babusci, D. Badoni, I. Balwierz-Pytko et al., Limit on the production of a light vector gauge boson in meson decays with the KLOE detector, Physics Letters B, vol. 720, no. 13, pp. 111 115, 2013.

[22] P. Adlarson, W. Augustyniak, W. Bardan et al., Search for a dark photon in the 0 e+ e decay, Physics Letters B, vol. 726, no. 13, pp. 187193, 2013.

[23] J. D. Bjorken, R. Essig, P. Schuster, and N. Toro, New fixed- target experiments to search for dark gauge forces, Physical Review D, vol. 80, no. 7, Article ID 075018, 2009.

[24] S. Andreas, C. Niebuhr, and A. Ringwald, New limits on hidden photons from past electron beam dumps, Physical Review D, vol. 86, no. 9, Article ID 095019, 2012.

[25] J. Blumlein and J. Brunner, New exclusion limits for dark gauge forces from beam-dump data , Physics Letters B, vol. 701, no. 2, pp. 155159, 2011.

[26] S. N. Gninienko, Stringent limits on the 0 X, X e+ e decay from neutrino experiments and constraints on new light gauge bosons , Physical Review D, vol. 85, no. 5, Article ID 055027, 2012.

[27] S. N. Gninienko, Constraints on sub-GeV hidden sector gauge bosons from a search for heavy neutrino decays , Physics Letters B, vol. 713, no. 3, pp. 244248, 2012.

[28] M.J. Savage, B.W. Filippone, L.W. Mitchell, Phys. Rev. D37 (1988) 1134.

[29] F.W.N. de Boer *et al.*, Phy. Lett. B **388**, 235 (1996)0.

[30] F.W.N. de Boer *et al.* J. Phys. G **23**, L85 (1997).

[31] D.R. Tilley et al., Nucl. Phys. A745 (2004) 155.

[32] H. Daniel and W. Bothe, Naturforschung 9a (1954) 402.

[33] R. Bent. T. Bonner and R. Sippel, Phs. Rev. 98 (1955) 1237.

[34] D.E. Alburger, Rev. Sci Instr. 27 (1956) 991. DE. Alburger, Phys. Rev. 111 (1958) 1586.

[35] E.K. Warburton, D.E. A.lburger, A. Gailman, P. Wagner and L.F. Chase, .Jr.. Phys. Rev. Bt33 (1964) 42.

[36] J. Kjetlman and B. Jvhans,on, Ark. Fysik 14 (1958) 17.

[37] J.C. Adloff, K.H. Souv, D. Diadier, F. Scheibling, P. Chevallier aud Y. Wolfson, Phys. Rev. C10 (1974) 1819.

[38] M. Ulrickson, N. Benczer-Koller. J.R. MacDonald aud J.W. Tape, Phys. Rev. C15 (1977) 186.

[39] M. Birk, J.S. Sokolowski, Y. Wolfson and N. BenczerKolIer, Nuci. Iristr. and Meth. 203 (1982) 255.

[40] S. Schumann and M. Waldachmidt, Z. Physik 271 (1974) 97.

[41] M. Watdschnaidt and P. Osterman, Nuci. Jnstr. and Meth. 89 (1970) 65.

[42] A. Passoja, P. Tikkanen, A. Krasznahorkay, Z. Gácsi, T. Kibédi and T. Fényes, Nucl . Instr. and Meth. 223 (1984) 96.

[43] T. Kibédi et al., Nucl . Instr. and Meth. A294 (1990) 523.

[44] T. Kibédi et al., EPJ Web of Conferences 35 06001 (2012) (DOI: 10.1051/epj-conf/20123506001).

[45] Montoya et al., Nucl . Instr. and Meth. A334 (1993) 437.

[46] A. Buda, J.C.S . Bacelar, A. Balanda t, J . van Klinken, Z. Sujkowski z and A. van der Woude, Nucl . Instr. and Meth. A335 (1993) 479.

[47] K.E. Stiebing *et al.*, J. Phys. G **30**, 165 (2004).

[48] F. Sauli, Gaseous Radiation Detectors Fundamentals and Applications, Cambridge Monographs on Particle Physics, Nuclear Physics and Cosmology, (2014)

[49] Stephen Biagi. Magboltz: Transport of electrons in gas mixtures. http://consult.cern.ch/writeup/magboltz/.

[50] G. Charpak, R. Bouclier, T. Bressani, J. Favier and C. Zupancic, Nucl. Instr. and Meth. 62 (1968) 262

[51] G. Charpak, Annu. Rev. Nucl. Sci. 20 (1970) 195.

[52] P. Convert and J.B. Forsyth (eds), Position sensitive detection of thermal neutrons (Academic Press, London, 1983).

[53] G. Charpak and F. Sauli, Nucl. Instrum. Methods 162, 277 (1979).

[54] G. Aad et al., The ATLAS experiment at the CERN Large Hadron Collider, CERN preprint.

[55] Y. Giomataris. P. Rebourgeard, J.P. Robert and G. Charpak, Nucl. Instr. and Meth. A 376 (1996) 29.

[56] Y. Giomataris Development and prospects of the new gaseous detector "Micromegas" Nucl. Instr. Meth. A 419 (1998) 239.